

# SPECTROSCOPIC AND DFT INVESTIGATION OF BENZALDEHYDE ISONICOTINO – HYDRAZIDE COMPOUND

I.B. COZAR<sup>1</sup>, A. PÎRNĂU<sup>1</sup>, L. SZABO<sup>2</sup>, N. VEDEANU<sup>3</sup>, C. NASTASĂ<sup>3</sup>, O. COZAR<sup>2,4</sup>

<sup>1</sup>National Institute for Research and Development of Isotopic and Molecular Technologies,  
65-103 Donath, 400293 Cluj-Napoca, Romania, E-mail: bogdan.cozar@itim-cj.ro

<sup>2</sup>Babeş-Bolyai University, Faculty of Physics, RO-400084, Cluj-Napoca, Romania

<sup>3</sup>Iuliu Hatieganu University of Medicine and Pharmacy, Faculty of Pharmacy, RO-400023  
Cluj-Napoca, Romania, E-mail: nicoletavedeanu@yahoo.com

<sup>4</sup>Academy of Romanian Scientists, Splaiul Independenței 54, RO-050094, Bucharest, Romania

*Received February 5, 2016*

The potential antimicrobial compound aroyl-hydrazone 4-[2-(4-methyl-2-phenyl-thiazole-5-yl)-2-oxo-ethoxy]-benzaldehyde isonicotino – hydrazide (BINH) was synthesized and investigated by FT-IR, FT-Raman, <sup>1</sup>H-NMR methods and also by DFT calculations at B3LYP/6-31G(d) level of theory in order to elucidate some structural aspects. Very good correlation between the vibrational and theoretical data shows that the proposed optimized structure is very close to reality. The molecular electrostatic potential (MEP) of this molecule suggests a parallel adsorbed orientation on the silver nanoparticles by the oxygen atoms and the  $\pi$ -electrons of rings. NMR data show a monomeric behavior of this compound in DMSO-solutions.

*Key words:* isonicotinic compound, IR, Raman, NMR, DFT.

## 1. INTRODUCTION

The treatment of infectious diseases is an important and challenging problem due to a combination of factors, including emerging infectious diseases and the increasing number of multi-drug resistant microbial pathogens. Bacterial resistance has become a serious public health problem, demanding new classes of antibacterial agents [1, 2]. A potential approach to overcome the resistance problem may be represented by the design of innovative agents having a different mechanism of action, without any cross-resistance with the therapeutic agents already in use. Thiazoles and their derivatives have attracted the interest over the last decades because of their varied biological activities: antifungal, anti-inflammatory, anti-allergic [3–6].

The new aroyl-hydrazone [7], arylidene – thiazolidine [8, 9], pyridyl – thiazole [10] and thiazolidinedione [11] compounds as potential antimicrobial agents were synthesized and tested *in vitro* against various Gram-negative and Gram-positive bacteria for their pharmacological properties.

Structural investigations of potential biomedical and pharmacological compounds are very much developed in the last years on scientific literature. For this goal, experimental methods like FTIR, Raman, SERS, NMR and quantum chemical calculations based on density functional theory (DFT) were successfully used in order to a good understanding of their pharmacological activity [12–17].

The Cu(II), Ni(II) and Co(II) complexes of a new Schiff base of 2-aminobenzimidazole as antitumor, antioxidant and antimicrobial agents have also been synthesized and characterized by similar spectroscopic methods [18].

In this context, the structural investigations by vibrational spectroscopic methods (FTIR, Raman) and <sup>1</sup>H-NMR, as well as density functional theory (DFT) based calculations performed on the BINH molecule are reported in this paper.

To the best of our knowledge, assignment of the normal vibrational modes of this compound on IR and Raman spectroscopies coupled with quantum chemical calculations has not been done so far.

For a proper understanding of the IR and Raman spectra and a reliable assignment of all vibrational bands, DFT calculations, particularly those based on hybrid functional methods [19] have evolved to a powerful quantum chemical tool for the determination of the electronic structure of molecules. In this framework, the B3LYP hybrid exchange-correlation functional is one of the most used since it proved its ability in reproducing various molecular properties, including vibrational spectra. The combined use of B3LYP functional and standard split valence basis set 6-31G(d) has been previously shown [20, 21] to provide an excellent compromise between accuracy and computational efficiency of vibrational spectra for large and medium-size molecules.

## 2. EXPERIMENTAL

This compound was prepared by condensing of 4-[2-(4-methyl-2-phenylthiazole-5-yl)-2-oxo-ethoxy] – benzaldehyde derivative with isonicotinoyl hydrazide in refluxing acetic acid 50% [7]. Its purity was determined by thin layer chromatography (TLC) and the antimicrobial activity was tested *in vitro* against various Gram-negative and Gram-positive bacteria. It showed poor to moderate antimicrobial activity on Gram-negative strains, but none effect on Gram-positive bacteria.

FT-IR and FT-Raman spectra of BINH powder were recorded at room temperature on a conventional Equinox 55 (Bruker Optik GmbH, Ettlingen, Germany) FT-IR spectrometer, equipped with an InGaAs detector, coupled with a Miracle (PIKE Technologies) ATR sampling device with a single reflection ZnSe crystal plate as the internal reflection element. Before recording the FT-IR/ATR spectrum a background spectrum was recorded in order to eliminate the

absorptions of atmospheric water and carbon dioxide. A standard ATR intensity correction performed by the OPUS software was applied.

The FT-Raman spectrum of BINH was recorded in backscattering geometry with a Bruker FRA 106/S Raman accessory equipped with a nitrogen cooled Ge detector. The 1064 nmNd:YAG laser was used as excitation source, and the laser power measured at the sample was 300 nW. All IR and Raman spectra were recorded with a resolution of  $4\text{ cm}^{-1}$  by co-adding 32 scans.

The  $^1\text{H-NMR}$  spectrum of this new compound were recorded at room temperature on a Bruker Avance III NMR spectrometer operating at 500 MHz for  $^1\text{H}$ , all chemical shifts being measured relative to TMS. The samples were prepared by dissolving the synthesized powder of this compound (BINH) in  $\text{DMSO-d}_6$  ( $\delta_{\text{H}} = 2.512\text{ ppm}$ ). The spectrum was recorded using 32 scans collected into 65 K data points over a 7000 Hz spectral window and an excitation pulse of  $10.1\ \mu\text{s}$ .

### 3. RESULTS AND DISCUSSION

#### 3.1. IR SPECTRA

The B3LYP/6-31G(d) optimized geometry of studied compound is given in Fig. 1.

Experimental and calculated FT – IR spectra in the  $400\text{--}3200\text{ cm}^{-1}$  region are shown in Fig. 2.

Representative experimental FT-IR bands together with calculated wavenumbers and their assignments are given in Table 1.

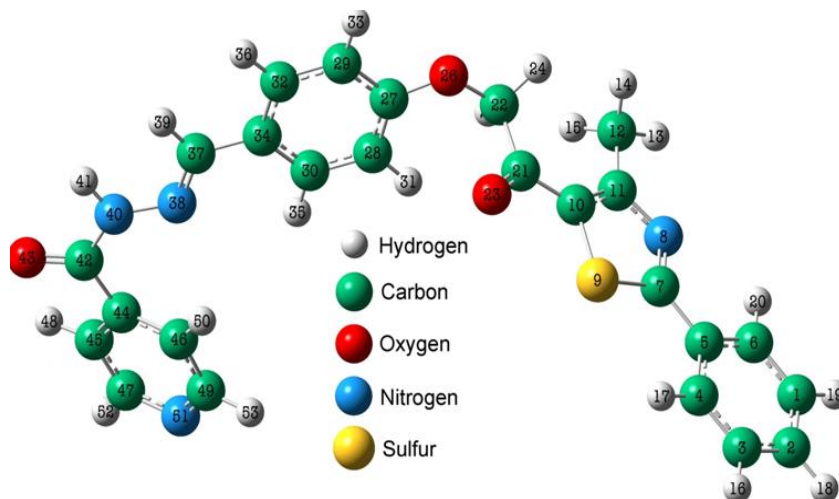


Fig. 1 – The B3LYP/6-31G(d) optimized geometry of 4-[2-(4-methyl-2-phenyl-thiazole-5-yl)-2-oxo-ethoxy]-benzaldehyde isonicotino – hydrazide (BINH).

The bands at 682  $\text{cm}^{-1}$  and 764  $\text{cm}^{-1}$  are due to the out of plane bending vibrations characteristics of CH and  $\text{CH}_3$  groups from rings 1,2 and 4, respectively.

A superposition between asymmetric stretching vibration of O26-C22-C21 group with the in plane deformations of rings 2,3 and CH groups is at 804  $\text{cm}^{-1}$ . The out of the plane bending vibrations characteristic to CH groups from ring 3 appear at 847  $\text{cm}^{-1}$  and 1169  $\text{cm}^{-1}$ .

Table 1

Selected experimental FT-IR bands together with calculated wavenumbers and their assignments

Experimental wavenumbers ( $\text{cm}^{-1}$ )		Calculated wavenumbers ( $\text{cm}^{-1}$ )	
FTIR/ATR	FTIR	B3LYP	Band assignment
3029	3028	3054	$\nu(\text{CH ring4})$
1668	1669	1694	$\nu_s(\text{CO43}), \delta(\text{N40H})$
1654	1655	1684	$\nu_s(\text{CO23}), \delta(\text{C22H}_2)$
1606	1610	1600	$\nu(\text{CC ring3}), \delta(\text{CH ring3}), \nu(\text{CN38}), \delta(\text{C37H})$
1552	1552	1548	$\nu_{\text{as}}(\text{CC, CN ring4}), \delta(\text{CH ring4})$
1507	1508	1506	$\nu_{\text{as}}(\text{CC ring3}), \delta(\text{CH ring3})$
1453	1453	1462	$\nu(\text{N40C, N-N}), \delta(\text{C37H, N40N})$
1415	1417	1410	$\nu(\text{CC, CN ring2}), \delta(\text{CH ring1, ring2; CH}_3)$
1321	1323	1323	$\nu_{\text{as}}(\text{CC ring3}), \delta(\text{CH ring4, ring3; NH, CH, CH}_2, \text{CH}_3)$
1304	1306	1306	$\nu_{\text{as}}(\text{CC, CN ring3, ring4}), \delta(\text{CH ring4, ring3; NH, CH, CH}_2)$
1289	1290	1292	$\nu(\text{CC ring3, ring1}), \delta(\text{CH ring3, ring1})$
1259	1260	1270	$\delta(\text{CH}_2, \text{CH ring3}), \nu(\text{O26C, CC ring3})$
1246	1247	1227	$\delta(\text{CH}_2); \text{ring1, ring2, ring3 breathing}; \delta(\text{CH ring3, ring1})$
1169	1169	1160	$\delta(\text{CH ring3})$
1062	1063	1073	$\nu_{\text{as}}(\text{O26-C22-C21}), \text{ip. (ring3) deformation}, \delta(\text{CH ring3, ring1})$
1015	1014	1031	$\text{ip. (ring2) deformation}, \delta(\text{CH}_3), \delta(\text{CH ring1})$
949	949	957	$\text{ring1, ring2 breathing}; \delta(\text{CH ring1, ring2}), \delta(\text{CH}_2, \text{CH}_3)$
847	847	844	$\text{op. bending (CH ring3)}$
804	804	791	$\nu_{\text{as}}(\text{O26-C22-C21}), \text{ip. (ring3, ring2) deformation}, \delta(\text{CH ring3, ring2}), \delta(\text{CH}_2, \text{CH}_3)$
764	765	768	$\text{op. bending (CH ring4)}$
682	684	672	$\text{op. bending (ring2, ring1), op. bending (CH ring1, CH}_3)$

$\nu$  – stretching,  $\delta$  – in-plane bending, op. – out of plane and ip. – in plane deformations, ring1 (benzene C1-C6), ring2 (C7-N8-C11-C10-S9), ring3 (benzene C27-C34), ring4 (piridyne)

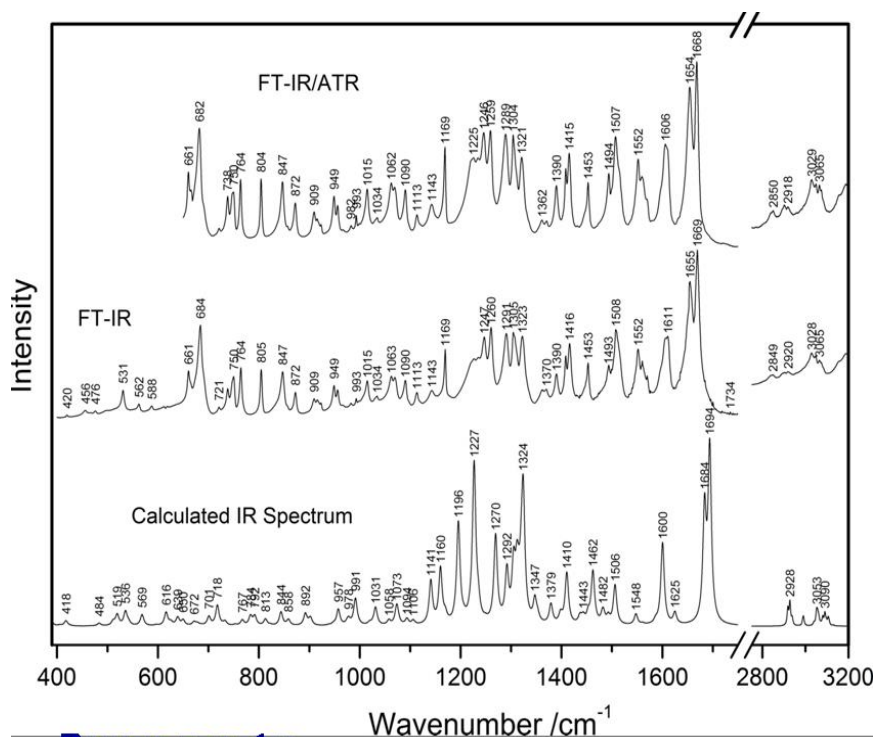


Fig. 2 – Experimental FTIR and calculated IR spectra of the investigated compound.

A superposition between breathing vibrations of rings 1, 2 and 3 with deformation vibrations of  $\text{CH}_2$  group appears at  $1246 \text{ cm}^{-1}$ . Another superposition of bending  $\text{CH}$ ,  $\text{CH}_2$  vibrations and  $\text{O}26\text{-C}$ ,  $\text{C-C}$  stretching vibrations from ring 3 is at  $1259 \text{ cm}^{-1}$ . The three bands  $1289 \text{ cm}^{-1}$ ,  $1304 \text{ cm}^{-1}$ ,  $1321 \text{ cm}^{-1}$  are due to the superposition of stretching vibrations ( $\nu$ ,  $\nu_{\text{as}}$ ) of  $\text{C-C}$ ,  $\text{C-N}$  groups from rings 1, 3, 4 with bending vibrations of  $\text{CH}$  groups of the same rings and of other  $\text{CH}$ ,  $\text{NM}$ ,  $\text{CH}_2$ ,  $\text{CH}_3$  groups.

The band from  $1453 \text{ cm}^{-1}$  is due to the complex superposition of stretching  $\text{N}40\text{C}$ ,  $\text{N}40\text{N}$  vibrations with bending  $\text{C}37\text{H}$ ,  $\text{N}40\text{H}$  vibrations. Other superpositions between asymmetric stretching  $\text{CC}$ ,  $\text{CN}$  vibrations with bending  $\text{CH}$  vibrations of rings 3 and 4 are evidenced at  $1507 \text{ cm}^{-1}$  and  $1552 \text{ cm}^{-1}$ , respectively. A superposition of stretching  $\text{CC}$  ring 3 and  $\text{C-N}38$  vibrations with bending  $\text{CH}$  ring 3 and  $\text{C}37\text{H}$  vibrations is at  $1606 \text{ cm}^{-1}$ .

The two intense bands from  $1654 \text{ cm}^{-1}$  and  $1668 \text{ cm}^{-1}$  are due to the superposition of symmetric stretching vibrations of  $\text{CO}23$  and  $\text{CO}43$  groups with bending  $\text{C}22\text{H}_2$  and  $\text{N}40\text{H}$  vibrations, respectively.

The last band from  $3029\text{ cm}^{-1}$  is assigned to stretching vibrations of CH groups from ring 4.

### 3.2. RAMAN SPECTRA

Experimental and calculated Raman spectra of the investigated molecule are shown in Fig. 3. The most intense Raman bands, experimental and calculated, together with their assignments are given in Table 2.

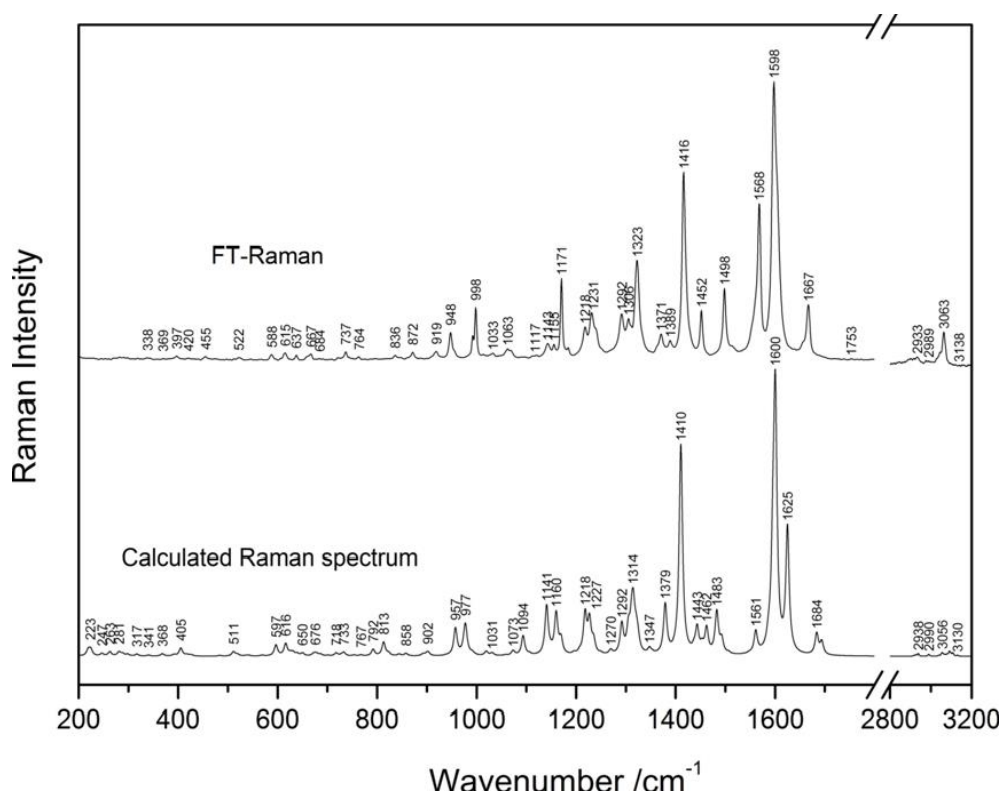


Fig. 3 – Experimental FT-Raman and calculated Raman spectra of BINH compound.

The superposition of breathing ring 1 and ring 2 vibrations with bending vibrations of CH groups from these rings appear at  $948\text{ cm}^{-1}$ . The  $998\text{ cm}^{-1}$  and  $1171\text{ cm}^{-1}$  bands are assigned to ring 1 breathing vibrations and bending CH ring 3 vibrations, respectively. An overlap of CH bending vibrations from rings 1, 2, 4 with those of CH,  $\text{CH}_2$ ,  $\text{CH}_3$  groups and also of stretching CC, CN groups from ring 2 with bending vibrations of CH rings 1, 2 groups appear at  $1323\text{ cm}^{-1}$  and  $1416\text{ cm}^{-1}$ , respectively.

The 1452  $\text{cm}^{-1}$  band is due to the overlap between stretching N40C, N-N vibrations with bending C37H, N40H vibrations. The in plane ring 1, ring 2 deformations overlapped with bending  $\text{CH}_2$ ,  $\text{CH}_3$  vibrations appear at 1498  $\text{cm}^{-1}$ .

The two intense bands from 1568  $\text{cm}^{-1}$  and 1598  $\text{cm}^{-1}$  are due to the superimposed of stretching CC ring 3 vibrations with bending CH ring 3 vibrations.

The 1667  $\text{cm}^{-1}$  band is assigned to symmetric stretching CO23 vibrations and bending C22H<sub>2</sub> vibrations.

The last 3063  $\text{cm}^{-1}$  band is due to stretching CH ring 4 vibrations.

Table 2

Selected experimental FT-Raman bands together with calculated wavenumbers and their assignments

Experimental wavenumbers ( $\text{cm}^{-1}$ )	Calculated wavenumbers ( $\text{cm}^{-1}$ )	
FT-Raman	B3LYP	Band assignment
3063	3056	$\nu(\text{CH ring4})$
1667	1684	$\nu_s(\text{CO23}), \delta(\text{C22H}_2)$
1598	1600	$\nu(\text{CC ring3}), \delta(\text{CH ring3}), \nu(\text{CN38}), \delta(\text{C37H})$
1568	1561	$\nu_s(\text{CC ring3}), \delta(\text{CH ring3}), \nu(\text{CN38})$
1498	1483	ip. (ring1, ring2) deformation, $\delta(\text{CH}_3 \text{ CH}_2), \delta(\text{CH ring1})$
1452	1462	$\nu(\text{N40C, N-N}), \delta(\text{C37H, N40N})$
1416	1410	$\nu(\text{CC, CN ring2}), \delta(\text{CH ring1, ring2; CH}_3)$
1371	1379	$\delta(\text{CH}_3, \text{CH}_2)$
1323	1314	$\delta(\text{CH ring1, ring4, ring2; CH, CH}_2, \text{CH}_3)$
1231	1226	$\delta(\text{CH}_2); \text{ring1, ring2, ring3 breathing; } \delta(\text{CH ring3, ring1})$
1171	1160	$\delta(\text{CH ring3})$
998	977	ring1 breathing
948	958	ring1, ring2 breathing; $\delta(\text{CH ring1, ring2}), \delta(\text{CH}_2, \text{CH}_3)$

$\nu$  – stretching,  $\delta$  – in-plane bending, op. – out of plane and ip. – in plane deformations, ring1 (benzene C1-C6), ring2 (C7-N8-C11-C10-S9), ring3 (benzene C27-C34), ring4 (pyridine)

### 3.3. MOLECULAR ELECTROSTATIC POTENTIAL (MEP)

Molecular electrostatic potentials have been used extensively for interpreting and predicting the reactive behavior of a wide variety of chemical systems in both

electrophilic and nucleophilic reactions, the study of biological recognition processes and hydrogen bonding interactions [14, 18].

To predict reactive sites for electrophilic and nucleophilic attack for the investigated compound, molecular electrostatic potential (MEP) was calculated at the B3LYP/6-31G(d) optimized geometries.

Figure 4 shows the calculated surface mapped 3D electrostatic potential in [a.u.], the electron density isosurface being 0.02 a.u.

The negative regions are related to electrophilic reactivity and the positive ones to nucleophilic reactivity. As can be seen in Figure 4, this molecule has several negative regions associated with O23, O26, O43 and N51 atoms. The most negative value of  $-0.1031$  a.u. is associated with O23, O26 atoms while the values for O43 and N51 are about  $-0.0822$  a.u., and  $-0.07146$  a.u., respectively. Thus, it would be predicted that an electrophile will preferentially attack this molecule at the O23, O26 positions and then the positions O43, N51.

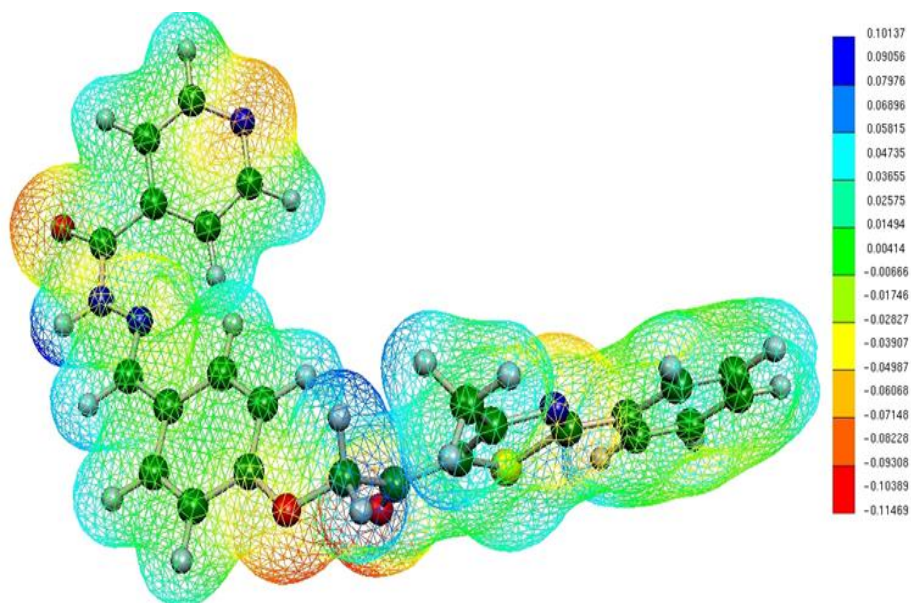


Fig. 4 – B3LYP/6-31G(d) calculated 3D electrostatic potential contour map of the studied molecule (a.u.).

Alternatively, we found a maximum value of  $0.04735$  a.u. on the  $\text{CH}_2$  and  $\text{CH}_3$  groups region indicating that these sites can be the most probably involved in nucleophilic processes.

The MEP of this molecule suggests also a parallel adsorbed orientation on the silver nanoparticles by the oxygen atoms and the  $\pi$  – electrons of rings.

## 3.4. NMR SPECTRUM

The  $^1\text{H}$  – NMR measurements on the investigated compound were performed on liquid state samples, using  $\text{DMSO-}d_6$  as deuterated solvent (gives a residual peak of water at about 3.37 ppm [22] in  $^1\text{H}$  NMR spectrum). For NMR spectrum (Fig. 5) discussion the atom numbering scheme presented in Fig. 1 was used.

The aromatic rings protons give signals in 7–9 ppm range: H17 and H20 multiplet at 8.052 ppm; H16, H18 and H19 multiplet at 7.577 ppm; H31 and H33 doublet at 7.123 ppm; H35 and H36 doublet at 7.714 ppm; H48 and H50 doublet at 7.824 ppm; H52 and H53 doublet at 8.789 ppm. The singlet peak at 11.995 ppm is assigned to H41 and the singlet peak at 8.420 ppm is assigned to H39. The protons of the methylene group give signals to 5.435 ppm and the protons of the methyl group appear at 2.785 ppm. The values of peak integrals nicely reproduce the number of protons from each group.

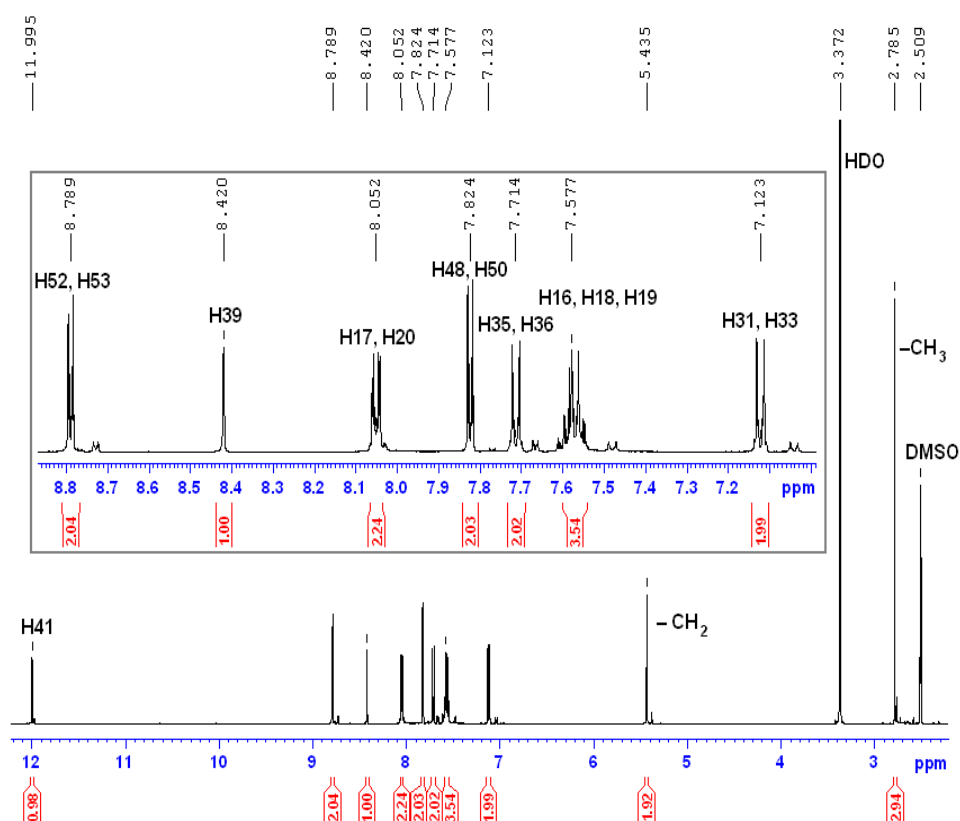


Fig. 5 –  $^1\text{H}$  NMR spectrum of BINH molecule; inset: details zoom to 7–9 ppm.

#### 4. CONCLUSIONS

Vibrational FT-IR, FT-Raman and NMR spectroscopies and also DFT calculations were successfully used to obtain the structural details on a potential antimicrobial isonicotino-hydrazide compound.

All the representative experimental vibrational bands were assigned in agreement with theoretical calculations at B3LYP/6-31G(d) level of theory.

The very good correlation between experimental and theoretical data suggests that the optimized molecular structure is very close to reality.

The calculated surface mapped 3D electrostatic potential predict the electrophilic and nucleophilic reactive attack sites for the investigated molecule and also its possible orientation adsorbed on the silver nanoparticles.

Also the NMR spectrum shows a monomeric behaviour of this compound in solutions.

*Acknowledgements.* Financial support from the National Authority for Scientific Research and Innovation – ANCSI, Core Programme, Project PN16-300203 is gratefully acknowledged.

#### REFERENCES

1. C. Franchini, M. Muraglia, F. Corbo, M. A. Florio, A. Di Mola, A. Rosato, R. Matucci, M. Nesi, F. van Bambeke, C. Vitali, *Arch. Pharm. Chem. Life Sci.*, **342**, 605 (2009).
2. Y. Özkay, Y. Tunalı, H. Karaca, I. Işıkdag, *Arch. Pharm. Chem. Life Sci.*, **11**, 264 (2011).
3. H. S. Sader, D. M. Johnson, R. N. Jones, *Antimicrob. Agents and Chemother.*, **48** (1) 53 (2004).
4. M. Kurazono, I. Takashi, K. Yamada, Y. Hirai, T. Maruyama, E. Shitara, M. Yonezawa, *Antimicrob. Agents and Chemother.*, **48**, 2831 (2004).
5. A. De Logu, M. Saggi, M. C. Cardia, R. Borgna, C. Sanna, B. Saggi, E. Maccioni, *J. Antimicrob. Chemother.*, **55**, 692 (2005).
6. C.M. Moldovan, O. Oniga, A. Pârvu, B. Tîperciuc, Ph. Verité, A. Pîrnău, O. Crişan, M. Bojiţă, R. Pop, *Eur. J. Med. Chem.*, **46**, 526 (2011).
7. C. Moldovan, O. Oniga, R. Meda, B. Tîperciuc, Ph. Verité, A. Pîrnău, O. Crişan, M. Bojiţă, *Farmacia*, **59**, 659 (2011).
8. A. Stana, B. Tîperciuc, M. Duma, L. Vlase, O. Crişan, A. Pîrnău, O. Oniga, *J. Heterocyclic Chem.*, **51**, 411 (2014).
9. A. Stana, B. Tîperciuc, M. Duma, A. Pîrnău, Ph. Verité, O. Oniga, *J. Serb. Chem. Soc.*, **79**, 115 (2014).
10. S. Oniga, M. Duma, O. Oniga, B. Tîperciuc, A. Pîrnău, C. Aramiciu, M. Palage, *Farmacia*, **63**, 171 (2015).
11. C. Nastasă, B. Tîperciuc, A. Pârvu, M. Duma, I. Ionuţ, O. Oniga, *Arch. Pharm. Chem. Life Sci.*, **346**, 481 (2013).
12. M. Baia, S. Astilean, T. Iliescu, *Raman and SERS Investigations of Pharmaceuticals*, Springer-Verlag, Berlin, 2008.
13. N. Leopold, *Surface Enhanced Raman Spectroscopy – Selected Applications*, Ed. Napoca Star, 2009.

14. N. Beckmann, R. Kneuer, H.U. Gremlich, H. Karmouty-Quintana, F.X. Blé, M. Müller, *NMR in Biomedicine*, **20**, 154 (2007).
15. L. Szabó, V. Chiş, A. Pîrnău, N. Leopold, O. Cozar, Sz. Orosz, *J. Mol. Struct.*, **924-926**, 385 (2009).
16. A. Pîrnău, V. Chiş, L. Szabo, O. Cozar, M. Vasilescu, O. Oniga, R.A. Varga, *J. Molec. Struct.*, **924-926**, 361 (2009).
17. A. Pîrnău, M. Bogdan, M. Mic, M. Palage, R.A. Varga, *Rom. Journ. Phys.*, **59**, 550 (2014).
18. N. El-wakiel, M. El-Weiy, M. Gaber, *Spectrochimica Acta Part A: Molec. Biomolec. Spectr.*, **147**, 117 (2015).
19. R.G. Parr, W. Yang, *Density-functional Theory of Atoms and Molecules*, Oxford University Press, New York, 1989.
20. I.B. Cozar, L. Szabo, N. Leopold, V. Chiş, O. Cozar, L. David, *J. Molec. Struct.*, **993**, 308 (2011).
21. L. Szabo, K. Herman, N.E. Mircescu, A. Fălămaş, L.F. Leopold, N. Leopold, C. Buzumurgă, V. Chiş, *Spectrochim. Acta*, **A93**, 266 (2012).
22. H.E. Gottlieb, V. Kotlyar, A. Nudelman, *J. Org. Chem.*, **62**, 7512 (1997).